Received: 31 May 2022 | Revised: 22 August 2022 | Accepted: 29 August 2022

DOI: 10.1002/bit.28219

ARTICLE

BIOTECHNOLOGY AND BIOENGINEERING WILEY

Genome-wide CRISPR-Cas9 screen reveals a persistent null-hyphal phenotype that maintains high carotenoid production in *Yarrowia lipolytica*

Brian Lupish[1] | **Jordan Hall**[2] | **Cory Schwartz**[2] | **Adithya Ramesh**[2] | **Clifford Morrison**[2] | **Ian Wheeldon**[2,3]

[1]Department of Bioengineering, University of California, Riverside, California, USA

[2]Department of Chemical and Environmental Engineering, University of California, Riverside, California, USA

[3]Center for Industrial Biotechnology, University of California, Riverside, California, USA

Correspondence

Ian Wheeldon, Department of Chemical and Environmental Engineering, University of California, Riverside, California, USA.
Email: wheeldon@ucr.edu

Present address

Cory Schwartz, iBio Inc., San Diego, California, USA.

Funding information

U.S. Department of Energy; National Science Foundation

Abstract

Yarrowia lipolytica is a metabolic engineering host of growing industrial interest due to its ability to metabolize hydrocarbons, fatty acids, glycerol, and other renewable carbon sources. This dimorphic yeast undergoes a stress-induced transition to a multicellular hyphal state, which can negatively impact biosynthetic activity, reduce oxygen and nutrient mass transfer in cell cultures, and increase culture viscosity. Identifying mutations that prevent the formation of hyphae would help alleviate the bioprocess challenges that they create. To this end, we conducted a genome-wide CRISPR screen to identify genetic knockouts that prevent the transition to hyphal morphology. The screen identified five mutants with a null-hyphal phenotype—*ΔRAS2*, *ΔRHO5*, *ΔSFL1*, *ΔSNF2*, and *ΔPAXIP1*. Of these hits, only *ΔRAS2* suppressed hyphal formation in an engineered lycopene production strain over a multiday culture. The *RAS2* knockout was also the only genetic disruption characterized that did not affect lycopene production, producing more than 5 mg L^{-1} OD^{-1} from a heterologous pathway with enhanced carbon flux through the mevalonate pathway. These data suggest that a *ΔRAS2* mutant of *Y. lipolytica* could prove useful in engineering a metabolic engineering host of the production of carotenoids and other biochemicals.

KEYWORDS

genetic screening, lycopene, metabolic engineering, nonconventional yeast, *RAS2*

1 | INTRODUCTION

Nonconventional filamentous and dimorphic fungi are of growing interest for bioproduction due to their abilities to metabolize a range of carbon sources and to produce biomolecules with high titers. One such fungus is *Yarrowia lipolytica*, an oleaginous dimorphic yeast that has desirable traits for industrial applications (Abdel-Mawgoud et al., 2018; Löbs et al., 2017; Zhu and Jackson, 2015). It is well suited for lipid biosynthesis, the production of fatty acids, carotenoids, and other acetyl-CoA-derived molecules (Blazeck et al., 2014; Morgunov et al., 2004; Schwartz, Frogue, Misa et al., 2017; Wang et al., 2022; Xue et al., 2013), and advanced genome editing tools are

Brian Lupish and Jordan Hall contributed equally to this study.

available to enable rapid pathway and strain design (Baisya et al., 2022; Ramesh et al., 2020; Schwartz et al., 2018; Schwartz, Frogue, Ramesh et al., 2017). Despite these successes, a number of technical challenges must be overcome before *Y. lipolytica* can be more widely used in industrial bioprocessing (Czajka et al., 2018; Sabra et al., 2017). Among these challenges are the obstacles posed by dimorphism and hyphal formation (Worland et al., 2020).

Hyphae are filamentous multicellular structures with contiguous parallel cell walls separated by septa, structures that form in multiple types of fungi including several budding yeasts (Crampin et al., 2005; Kiss et al., 2019). While the formation of hyphae is a default state for many fungal species, several yeasts including *Y. lipolytica* are dimorphic, that is, they are able to exist in a single cell free-floating state as well as a hyphal or pseudohyphal state (Ruiz-Herrera and Sentandreu, 2002; Vallejo et al., 2013). Transition into a hyphal or pseudohyphal state may result as a response to stressors such as starvation, high temperature, high pH, or low concentrations of dissolved oxygen (Bellou et al., 2014; Cullen and Sprague, 2000; Gimeno et al., 1992; Kawasse et al., 2003; Lee and Elion, 1999; Ruiz-Herrera and Sentandreu, 2002; Sudbery et al., 2004; Szabo, 1999). Although some bioproduction strategies benefit from hyphal morphology (Fickers et al., 2009), hyphal formation in a bioreactor can be problematic due to reduced mass transfer of dissolved oxygen and nutrients, increased culture viscosity, or increased stress response due to hyphal shearing (Ahamed and Vermette, 2010; Cai et al., 2014; Harvey and McNeil, 1994; Martin and Bushell, 1996; Müller et al., 2003; Z. J. Li et al., 2002). Hyphal growth is also associated with lower biosynthetic activity and product yields in some yeasts including ethanol from *Saccharomyces cerevisiae* (Reis et al., 2013) and lipid accumulation in *Y. lipolytica* (Bellou et al., 2014; Gajdoš et al., 2016). Therefore, it would be beneficial to engineer a null-hyphal phenotype strain of *Y. lipolytica*.

Compared to filamentous fungi, yeasts have fewer hyphae generating pathways and a simplified process of formation (Kiss et al., 2019). In addition, the transition from unicellular to hyphae often terminates in pseudo-hyphal morphology, with some yeasts never forming true hyphae (Berman and Sudbery, 2002; Pomraning et al., 2018). Nevertheless, the yeast-to-hyphae transition in dimorphic yeast still functions as a survival mechanism in nutrient-limited or stressful environments (Pomraning et al., 2018). While the full process of the yeast-to-hyphal transition is not completely understood in *Y. lipolytica*, two types of signaling cascades are known to be involved: two mitogen activated phosphorylation kinase (MAPK) cascades and a protein kinase A (PKA) pathway, both of which share notable conservation across dimorphic yeasts (Gancedo, 2001; Tisi et al., 2014). Despite the known relevance of these pathways in the yeast to hyphal transition, there remain many unidentified upstream and downstream components and poorly understood regulatory functions. Therefore, a broader coverage approach is needed to identify viable genetic targets for a null-hyphal phenotype.

Here, we used a pooled CRISPR-Cas9 knockout screen to identify null-hyphal knockout candidates in *Y. lipolytica*; several phenotypic knockouts were identified by selection of colonies with a smooth appearance, which is indicative of a loss of hyphal formation. We subsequently characterized the knockout strains' growth rates and retention of the null-hyphal phenotype. In doing so, we identified *RAS2* disruption as the most promising for industrial use. Finally, we tested the knockout's effect on lycopene production, demonstrating production without a loss of product titer in a strain devoid of hyphae.

2 | MATERIALS AND METHODS

2.1 | Strains construction

All strains were derived from *Y. lipolytica* PO1f (*MatA*, *leu2-270*, *ura3-302*, *xpr2-322*, *axp-2*). The Cas9 strain used in the genome-wide screen and growth assays was created by integrating a codon optimized copy of *CAS9* from *S. pyogenes* into the *A08* locus of *Y. lipolytica* by markerless integration. As described in (Schwartz et al., 2019), the genome copy of *CAS9* was expressed using a UAS1B8-TEF(136) promoter (Blazeck et al., 2011) with a ScCYC terminator. PO1f-HMEBI, the lycopene overproduction strain, was engineered as previously described in (Schwartz, Shabbir-Hussian et al., 2017). Briefly, the *HMG1*, *MVD1*, *CrtE*, *CrtB*, and *CrtI* were integrated in the genome as follows: two copies of *HMG1* were inserted, one into *D17* site and a second into the *XDH* site; one copy of *MVD1* was inserted into the disabled *LEU2* site, one copy of *CrtE* was inserted into the *A08* locus; one copy of *CrtB* was inserted into the *AXP* locus, and one copy of *CrtI* was inserted into the *XPR2* site. In addition to these insertions, the leucine and uracil auxotrophies were alleviated by randomly integrating function copies of the *Y. lipolytica* *LEU2* and *URA3* genes.

2.2 | Media and culture conditions

Unless otherwise noted, all *Y. lipolytica* strains were culture YPD media (1% Bacto yeast extract, 2% Bacto peptone, 2% glucose). For the genome-wide screen and *RAS2* rescue assays, cell were grown in synthetic defined SC Leucine Deficient media (0.17% Yeast Nitrogen Base, 0.2% Leu deficient amino acid mix (5.6% of all 19 L-amino acids except for Leucine, 5.6% inositol, 5.6% uracil, 1.3% adenine, and 1.3% para-aminobenzoic acid), 0.5% Ammonium Sulfate). When grown for lycopene biosynthesis, we used YPD10 media (1% Bacto yeast extract, 2% Bacto peptone, 10% glucose). All *Y. lipolytica* cultures were conducted in 25 ml of media in 250 ml baffled shake flasks at 30°C and 225 rpm, inoculated to an OD_{600} of 0.1 using an overnight starter culture. All *Y. lipolytica* transformations as previously described (Schwartz et al., 2019; Schwartz, Frogue, Misa et al., 2017; Schwartz, Shabbir-Hussian et al., 2017).

DH5α *E. coli* cells were used to clone and propagate the plasmids used in the whole genome screen and subsequent gene knockouts. NEB TOP10 *E. coli* cells were used to clone and propagate the

plasmids used in the *RAS2* rescue assay. All *E. Coli* cultures were grown in Lysogeny Broth (1% Tryptone, 0.5% Yeast Extract, 1% NaCl) with 100 mg/L ampicillin for selective pressure.

2.3 | CRISPR-Cas9 screening for null-hyphal phenotypes

To screen for genetic knockouts that lack hyphal morphology we generated upward of 50,000 colonies representing members of the genome-wide knockout library. This library was previously generated (see Schwartz et al., 2019) and includes the functional disruption of more than 94% of all protein coding sequences in the PO1f strain. All colonies with a smooth phenotype (indicative of a loss of hyphal morphology) were visually identified and subjected to colony PCR. Sequencing of the CRISPR plasmids contained in each hit revealed five unique hits—YALI1_E35305g, YALI1_D05956g, YALI1_D30097g, YALI1_E30639g, and YALI_F04690g.

2.4 | Mutant strain growth rate

Each of the five null-hyphal mutants identified in the genome wide screen were characterized in terms of growth rate in shake flask cultures. Growth rates were determined by linearizing the mean OD values via natural logarithm calculations and subsequent linear regression, generating a slope representative of the growth rate.

2.5 | Plasmid construction

To generate genetic knockouts in the lycopene overexpression strain, we digested pCRISPRyl (Addgene #70007) with AvRII and then integrated a double stranded sgRNA insert targeting one of the following genes, *RAS2*, *RHO5*, *SFL1*, and *MHY1*. We generated the sgRNA inserts by annealing complementary oligos, and integrated each insert into the pCRISPRyl linearized backbone via Gibson assemblies. To rescue *RAS2* function, we replaced the *hrGFP* ORF in pIW209 with the *RAS2* ORF cloned from wild type PO1f genomic DNA via Golden Gate Assembly. All guide sequences and primers used here are provided in Supporting Information: Tables S1 and S2.

2.6 | Hyphal phenotype characterization

To measure the prevalence of hyphal phenotypes, the four generated PO1f-HMEBI knockouts (PO1f-HMEBI *ΔRAS2*, PO1f-HMEBI *ΔRHO5*, PO1f-HMEBI *ΔSFL1*, and PO1f-HMEBI *ΔMHY1*) were grown in duplicate for 10 days, along with PO1f and PO1f-HMEBI, which served as controls. On Days 1, 3, 6, 9, and 10, one slide from each duplicate of each strain was made using a 2 µl sample of the culture. Six photographs of each slide were taken (for a total of 12 photographs per strain per measurement day) with an Olympus BX51 Microscope on brightfield settings while using a 100x oil objective. ImageJ software was used to count the total number of cells in each image, and any cell with a length greater than twice its width was classified as exhibiting hyphal behavior.

2.7 | *RAS2* rescue assay

PO1f *ΔRAS2* was transformed with the *RAS2* rescue vector to generate a rescued RAS2 phenotype. PO1f and PO1f *ΔRAS2* were transformed with an empty vector to serve as positive and negative controls, respectively. Three millliters cultures of all three strains were grown overnight at 30°C. The next day, with the cultures in log phase, they were diluted to ODs of 0.2. A 4 ul droplet from all three dilutions was spotted onto a 1.2% Agar SC leucine deficient plate. The plate was grown for ~45 h, until the spots had matured. The spots were then photographed and their morphologies analyzed. Cells from each mutant were scraped from the plates and resuspended in 1 ml of SC leucine deficient media. A 2 µl sample of each solution was then visualized via confocal microscopy at 60x magnification.

2.8 | Lycopene quantification

Lycopene production cultures were grown as described in Schwartz, Frogue, Misa, et al. (2017), using 10% glucose media. Lycopene was extracted and quantified using a method detailed by Chen et al. (2016) for carotenoid extraction, with a few adaptations. At each measurement time point, triplicate 1 ml aliquots were withdrawn from each assay culture, and dry cell weights (DCW) of each were measured through centrifugation at 5000*g* for 3 min, media aspiration, and subsequent pellet drying at 80°C until stable weights were measurable. The pellets were then washed with water, repelleted, resuspended in 1 ml of 3 M HCl, and boiled for 2 min. The boiled pellets were then cooled in an ice bath for 3 min. After another water wash, the pellets were resuspended in 1 ml of acetone. 200 µl of 500–750 µm glass beads were added to each acetone resuspension, and the cells were lysed (while achieving liposome disruption) by vortexing the mixtures for 2 min. The resulting supernatant was collected, and lycopene titers were quantified by measuring the supernatant absorbance at 472 nm comparing measurements to a standard curve of purchased lycopene (Sigma-Aldrich); see Figure Supporting Information: S4.

3 | RESULTS AND DISCUSSION

To identify genes associated with hyphal formation, we used a pooled library of CRISPR-Cas9 sgRNAs to target nearly every gene in the genome of *Y. lipolytica* PO1f (Schwartz et al., 2019). The previously designed library covers 7854 coding sequences (CDS) with sixfold coverage. Unique sgRNAs were designed to target the first 300 exon

base pairs in each CDS, then scored and ranked based on their predicted on-target cutting efficiency (Doench et al., 2014). The final library contained the six highest scoring sgRNAs for each CDS, along with a negative control set of 480 nontargeting sgRNAs. Oligos encoding each sgRNA were commercially synthesized and subsequently cloned into an expression vector with sgRNA expression driven by a synthetic RNA polymerase III (Pol III) promoter (C. M. Schwartz et al., 2016), while Cas9 expression was accomplished through a genome-integrated expression cassette.

Multiday growth on solid media is often sufficient to trigger the transition from yeast to (pseudo)hyphal morphology, which can be readily observed by visual inspection because hyphae forming cells form a wrinkled or rough looking colony, while the absence of hyphae produce colonies with a smooth surface (Figure 1). To isolate strains deficient in hyphal formation, we plated *Y. lipolytica* PO1f transformed with the pooled library of sgRNA expression vectors and identified mature colonies with a smooth morphology. Colonies with this phenotype were isolated, restreaked, and the cellular phenotype was confirmed by microscopy. Sequencing of the sgRNA expression plasmids harbored in the isolated colonies, revealed five unique genes in cells with a putative null-hyphal phenotype, including functional disruptions to YALI_E35305g, D05956g, D30097g, E30639g, and F04690g (gene locus IDs based on CLIB89 annotation, the parent strain of PO1f (Magnan et al., 2016)).

Gene name and function of the morphology screen hits were identified through a BLASTp search, the results of which are shown in Supporting Information: Table S1. Notably, many of the screening hits correspond to a gene known to be associated with regulating cell morphology or cell stress: *RAS2* (YALI1_E35305g) encodes for a GTP binding protein involved in starvation response and cell morphology (Li et al., 2014; Mösch and Fink, 1997; Mösch et al., 1996); Sfl1 (encoded by YALI1_D05956g) bears similarity to known heat shock transcription factors (Pan and Heitman, 2002; Patterson et al., 2018); Snf2 (encoded by YALI1_D30097g) is a chromatin remodeling protein in the SWI/SNF transcription complex (Hirschhorn et al., 1992); and Rho5 (encoded by YALI1_E30639g) is involved in cell integrity, helping to propagate heat and oxidative stress signals leading to induced cell death. The final gene identified in our screen was (YALI_F04690g), whose encoded protein had a 40.9% uniprot BLAST identity score match with the Ptip protein (part of the histone H3K4 methyltransferase complex) in *Drosophila melanogaster* and is referred to here as *PAXIP1* (Fang et al., 2009).

A goal of this study was to identify one or more genetic knockouts that eliminate or suppress hyphal formation and that have minimal or no effect on the yeast's ability to perform as a biochemical production host. In addition to the resulting increase in time and resources required for a production run, a reduced growth rate can signify other metabolic burdens which may compromise the synthesis of the desired product. As such, we measured growth rates of the mutant strains (Figure 2) and observed that the *ΔRAS2*, *ΔRHO5*, and *ΔSFL1* strains had similar growth rates to unmodified PO1f, thus leaving these mutants as potential host candidates. The *ΔSNF2* and *ΔPAXIP1* strains, however, showed impeded growth, ruling out their use as potential null-hyphal hosts for industrial use. In addition to these mutants, we also characterized a *ΔMHY1* (YALI_B28150g) strain; Mhy1 functions downstream of Ras2, disruption of which has been shown to reduce hyphal formation without a reduced growth phenotype (Konzock and Norbeck, 2020; Morgunov et al., 2004). Given these results, the *ΔRAS2*, *ΔRHO5*, *ΔSFL1*, and *ΔMHY1* knockout strains were selected for further investigation.

With the growth rate of the hyphal knockout strains characterized, we proceeded to test the knockouts that had no effect on growth rate in a lycopene overproduction host. Previously, we reported a series of genetic manipulations to *Y. lipolytica* that introduce and enhance a lycopene biosynthesis pathway (Schwartz, Frogue, Misa et al., 2017; Schwartz, Shabbir-Hussain et al., 2017).

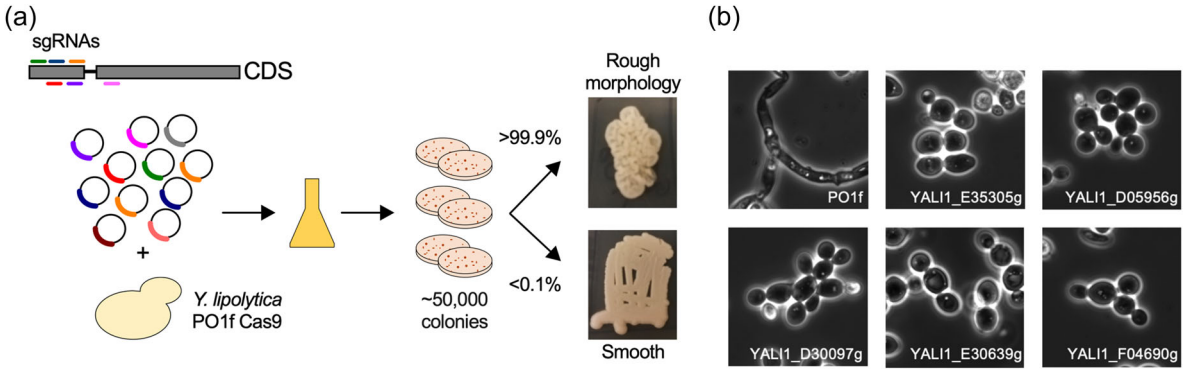

FIGURE 1 *Yarrowia lipolytica* genome-wide CRISPR-Cas9 morphology screen. (a) Six sgRNAs targeting each gene in the PO1f genome were designed, synthesized, and transformed as a pooled library. Transformed cells were plated on solid agar media and mature colonies were visually inspected after 4 days of growth. The vast majority of the cells presented with a rough or wrinkled morphology typical of *Y. lipolytica*. (b) AMicroscopy images of cells taken from colonies that presented with a smooth morphology are shown. A micrograph of PO1f cells forming hyphal structures is shown as a comparison to the putative null-hyphae mutants. Additional characterization PO1f and mutant cell morphology is shown in Figures 3, 4, and Supporting Information: S1, S2, and S3. YALI1_E35305g was identified as *RAS2*, YALI1_D05956g as *SFL1*, YALI1_D30097g as *SNF2*, YALI1_E30639g as *RHO5*, and YALI_F04690g as putatively *PAXIP1*.

These manipulations include the overexpression of a series of bacterial enzymes—CrtE, CrtB, and CrtI—that convert farnesyl pyrophosphate into lycopene, and the homologous overexpression of Hmg1 and Mvd1, both of which are known to increase mevalonate pathway flux to isopentenyl diphosphate, a precursor to lycopene biosynthesis. The lycopene production strain was designated as PO1f-HMEBI with each overexpression represented by H (*HMG1*), M (*MVD1*), E (*CrtE*), B (*CrtB*), and I (*CrtI*). Using PO1f-HMEBI as the parent strain, we generated the four most viable null-hyphal gene deletion candidates, *ΔRAS2*, *ΔRHO5*, *ΔSFL1*, and *ΔMHY1*, and characterized the percentage of cells that underwent a transition from yeast to hyphal morphology over a 10 day culture, a time course selected based on our experience in producing lycopene in engineered strains over a similar time period. At each time point, we withdrew an aliquot from two independent cultures, mounted the live samples on microscope slides, and generated six images per slide for a total of 12 images per strain per time point (examples provided in Supporting Information: Figure S1). We defined any cells with a length greater than twice the widest point as hyphal/pseudohyphal for the purposes of identifying all cells transitioning from the yeast state. Examples of both hyphal and pseudohyphal structures meeting this criteria are shown in Figure 3.

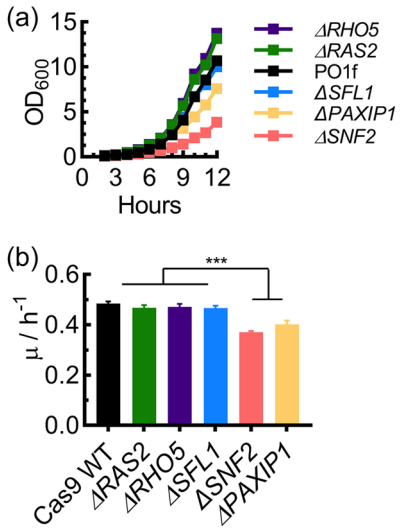

FIGURE 2 The effect of putative hyphal knockout on growth rate. (a) Time course of cell growth as measured by the optical density at 600 nm (OD_{600}). *Yarrowia lipolytica* cultures were grown in shake flask cultures with YPD media. (b) Growth rate, μ, calculated from the slopes of the natural logarithms of the growth curve measurements in part (a). Data points and bars represent the mean of triplicate measurements. Error bars represent the standard deviation. *** represents $p < 0.001$ from Dunnett's multiple comparisons test, post hoc of a one-way analysis of variance.

Both PO1f and PO1f-HMEBI showed hyphal transition behavior in approximately 15% of their cells across the full time series, establishing a baseline occurrence rate (Figure 4). *ΔRHO5* proved to be the least effective knockout with an ~3% hyphal occurrence after 1 day of culture, but jumping to ~20% after 3 days of growth and increasing to >28% after Day 9. Disruption of *SFL1* also resulted in early suppression of (pseudo)hyphal formation, maintaining ~5% elongated structures for 6 days of culture, increasing to >23% at Days 9 and 10. *ΔMHY1* began with ~3% hyphal occurrence, but steadily increased over subsequent days, reaching nearly 30% on Day 10. Unlike the other knockouts, *ΔRAS2* had low (<5%) hyphal occurrence across all 10 days, without the rebound of hyphal behavior noted in all of the other knockouts. We therefore identified *ΔRAS2* as the most promising benign and nontransient hyphal knockout generated.

One explanation for the lasting effect of the *RAS2* disruption is that Ras2 is an early control node for the transition to hyphal morphology, existing upstream of several hyphae-regulating pathways. Primarily responsive to glucose conditions outside the cell, Ras2 is a plasma-membrane GDP binding protein until being activated by Cdc25. Once activated, Ras2 has a broad cascade of interactions that lead to various stress responses through cyclic AMP and PKA as well as through the rho-like GTPase Cdc42, which in turn activates the MAPK pathway (M. Li et al., 2014; Mösch et al., 1996). The signal pathways modulated by the interaction of Ras2 and Cdc25 have been implicated in a wide range of downstream cellular processes, including transition to a filamentous state (Mösch and Fink, 1997). Ras2 is involved directly in sensing glucose in the environment and receives regulatory feedback from glucose metabolism through activation of Cdc25 by fructose-1-6-bisphosphate. Commonly acting to downregulate stress response genes, *RAS2* knockouts display a heightened basal stress tolerance in *S. cerevisiae*,

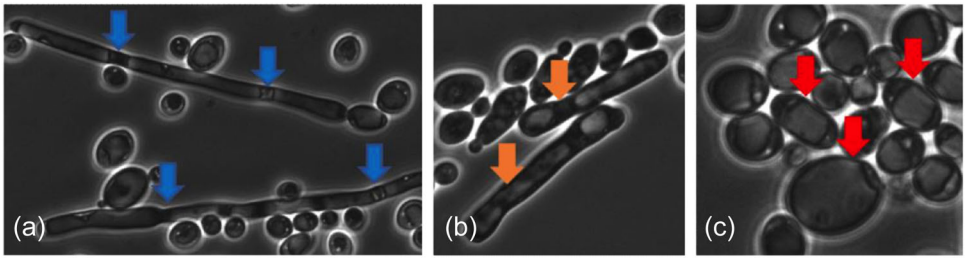

FIGURE 3 Images of hyphal, pseudohyphal, and budding phenotypes in *Yarrowia lipolytica*. (a) Image of the hyphal state, with blue arrows indicating septa between cells, which are characteristic of hyphae. (b) Image of the pseudohyphal state, with orange arrows indicating elongated cells with signs of incomplete division. (c) Image of the budding state, with red arrows pointing to unbranched and rounded yeast cells.

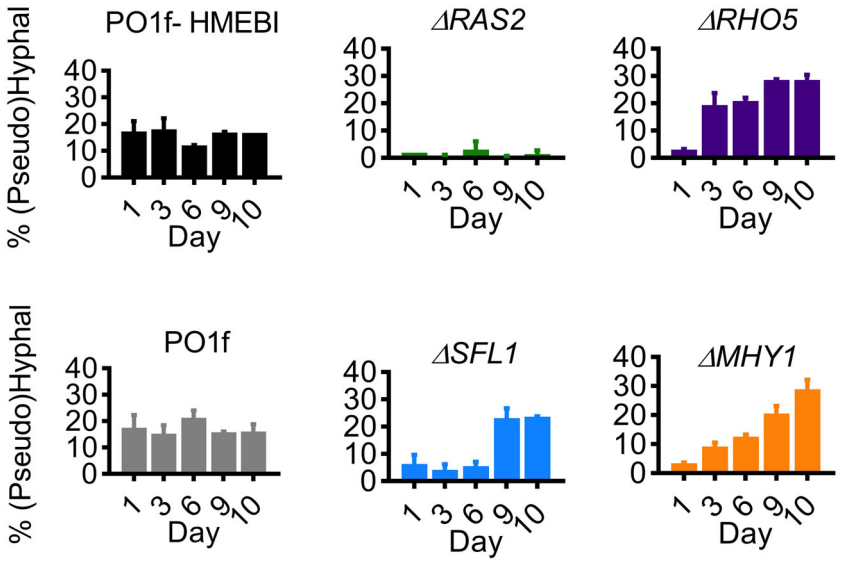

FIGURE 4 Hyphal morphology percentages of PO1f, PO1f-HMEBI, and putative hyphal knockout strains. The knockout strains include PO1f-HMEBI *ΔRAS2*, PO1f-HMEBI *ΔRHO5*, PO1f-HMEBI *ΔSFL1*, and PO1f-HMEBI *ΔMHY1*. Bars represent the average number of cells in a hyphal or pseudohyphal state observed in 12 different images across two biological replicates. At least 250 cells were characterized at each time point for each strain. Error bars represent the standard deviation across the 12 different images.

which is another industrially useful trait (Shama et al., 1998; Zacharioudakis et al., 2017). In this anticipatory state *RAS2* knockouts have shown greater thermotolerance and resistance to oxidative stress, while also exhibiting life span extension akin to that seen in response to calorie restriction. The *ΔRAS2* mutant is therefore a putative null hypal strain without other observed negative traits and some potentially unexpected potential benefits.

To ensure that Ras2 functions as a control node for hyphae formation, we conducted a rescue experiment with *RAS2* expressed from an episomal plasmid in a PO1f *ΔRAS2* strain. As shown in Figure 5, the rescued *ΔRAS2* cells regained the rough colony phenotype present in PO1f cells, as well as cellular filaments when viewed under a microscope. This indicates that the hyphae-forming wild type phenotype was restored in tandem with Ras2 expression, even as the *ΔRAS2* cells retained the null hyphal smooth colony phenotype. As such, we confirmed *RAS2* as a necessary gene for hyphal formation, where its presence has a direct relationship to the hyphal forming phenotype of *Y. lipolytica*.

A primary goal of this study was to identify genetic manipulations that reduce or eliminate hyphal formation in a production host. To this end, we generated *ΔRAS2*, *ΔRHO5*, *ΔSFL1*, and *ΔMHY1* mutant strains in a PO1f-HMEBI background and measured the effect of each knockout on lycopene production (Figure 6). As expected, the wild type HMEBI strain produced 2.8 mg of lycopene per gram of dry cell weight (mg/gDCW) by Day 3, and 4.9 or more mg lycopene/gDCW on Days 6 and 8, results equivalent to those previously reported for this strain (Schwartz, Frogue, Misa et al., 2017). The *ΔRHO5*, *ΔSFL1*, and *ΔMHY1* strains produced comparatively little lycopene, reaching 1.4 mg lycopene/gDCW or less by the end of an 8 day culture. The *ΔRAS2* strain, however, produced similar amounts of lycopene to the HMEBI strain, at 1.8 mg lycopene/gDCW on Day 3, around 4.0 mg lycopene/gDCW on Day 6, and 5.1 mg lycopene/gDCW on Day 8. It therefore functioned just as well as HMEBI as a lycopene production platform despite lacking the lycopene production enhancements of the HMEBI strain.

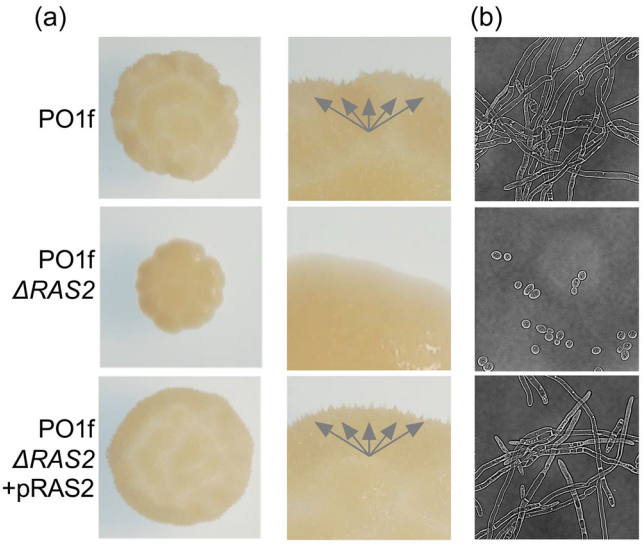

FIGURE 5 *ΔRAS2* rescue assay. (a) Rows represent different experimental groups, with the left column showing the full cell spot and the right column showing a magnified image of the top edge of the same spot. Both the wild type PO1f cells and the rescued *ΔRAS2* cells produced hyphal morphology with characteristic rough edges and hyphal structures, while the *ΔRAS2* knockout strain produced colonies with a smooth phenotype and round cells, indicative of a loss of the hyphal structures. Gray arrows indicate the rough or spiked edge indicative of hyphae. (b) Microscopy images of cells resuspended in liquid media. Samples are as indicated in (a).

While the *RAS2* knockout did not produce an increase in lycopene titer at the benchtop scale, the potential industrial benefits of its use cannot be overlooked. By eliminating hyphae formation in a fully functional production strain, associated labor costs and malfunctions from bioreactor fouling may be avoided, and cells that would have otherwise ended up on the bioreactor vessel could instead be harvested for more product. Likewise, the challenges of oxygen and nutrient diffusion due to the presence of hyphae is

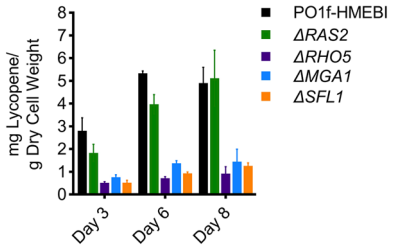

FIGURE 6 The effect of hyphal knockout on lycopene production in *Yarrowia lipolytica*. The HMEBI lycopene production strain and HMEBI *ΔRAS2* strain consistently produced two to four times as much lycopene as the HMEBI *ΔRHO5*, HMEBI *ΔSFL1*, and HMEBI *ΔMHY1* strains.

inherently worse in the large volumes of industrial bioreactors, where oxygen and nutrient diffusion is already a major challenge. It is even possible that an increased product titer could still be gained from a null-hyphal strain when grown at the scale of an industrial bioreactor through the reduction of low oxygen and nutrient regions in the vessel. Moreover, the known role of *RAS2* in the hyphal transition of *S. cerevisiae* and *Candida albicans* (Chow et al., 2019; Mösch and Fink, 1997; Parveen et al., 2019) speaks to the potential utility of this mutation for bioprocessing with other hosts. While more work must be done to quantify any theoretical titer increases from the *ΔRAS2* at an industrial scale, the practical value of a fully functional but lower maintenance strain should not be underestimated.

These results illustrate the utility of our CRISPR-Cas9 knockout library screen for identifying desirable phenotypes. Through a simple visual screen, we were able to rapidly identify and subsequently characterize a benign and industrially useful single gene knockout. Indeed, many industrially beneficial mutations have been and will continue to be identified through screens of whole genome knockout libraries. Furthermore, the knowledge we gain about what genes serve as effective regulatory and control points for our goals will inform future engineering in the next generation of bioproduction strains.

AUTHOR CONTRIBUTIONS

Cory Schwartz and Ian Wheeldon conceived the study. Cory Schwartz conducted the genetic screen. Jordan Hall and Brian Lupish created and characterized the genetic knockouts with the assistance of Adithya Ramesh and Clifford Morrison. All authors wrote and edited the paper.

ACKNOWLEDGMENT

This work was supported by NSF 1706545 and the U.S. Department of Energy (DOE) Joint Genome Institute (JGI) grant CSP-503076. The work conducted by the JGI, a DOE Office of Science User Facility, is supported under Contract No. DE-AC02-05CH11231.

DATA AVAILABILITY STATEMENT

The data that support the findings of this study are available from the corresponding author upon reasonable request.

ORCID

Ian Wheeldon http://orcid.org/0000-0002-3492-7539

REFERENCES

Abdel-Mawgoud, A. M., Markham, K. A., Palmer, C. M., Liu, N., Stephanopoulos, G., & Alper, H. S. (2018). Metabolic engineering in the host *Yarrowia lipolytica*. *Metabolic Engineering*, *50*, 192–208.

Ahamed, A., & Vermette, P. (2010). Effect of mechanical agitation on the production of cellulases by *Trichoderma reesei* RUT-C30 in a draft-tube airlift bioreactor. *Biochemical Engineering Journal*, *49*, 379–387.

Baisya, D., Ramesh, A., Schwartz, C., Lonardi, S., & Wheeldon, I. (2022). Genome-wide functional screens enable the prediction of high activity CRISPR-Cas9 and -Cas12a guides in *Yarrowia lipolytica*. *Nature Communications*, *13*, 922.

Bellou, S., Makri, A., Triantaphyllidou, I.-E., Papanikolaou, S., & Aggelis, G. (2014). Morphological and metabolic shifts of *Yarrowia lipolytica* induced by alteration of the dissolved oxygen concentration in the growth environment. *Microbiology*, *160*, 807–817.

Berman, J., & Sudbery, P. E. (2002). *Candida albicans*: A molecular revolution built on lessons from budding yeast. *Nature Reviews Genetics*, *3*, 918–930.

Blazeck, J., Hill, A., Liu, L., Knight, R., Miller, J., Pan, A., Otoupal, P., & Alper, H. S. (2014). Harnessing *Yarrowia lipolytica* lipogenesis to create a platform for lipid and biofuel production. *Nature Communications*, *5*, 3131.

Blazeck, J., Liu, L., Redden, H., & Alper, H. (2011). Tuning gene expression in *Yarrowia lipolytica* by a hybrid promoter approach. *Applied and Environmental Microbiology*, *77*, 7905–7914.

Cai, M., Zhang, Y., Hu, W., Shen, W., Yu, Z., Zhou, W., Jiang, T., Zhou, X., & Zhang, Y. (2014). Genetically shaping morphology of the filamentous fungus *Aspergillus glaucus* for production of antitumor polyketide aspergiolide A. *Microbial Cell Factories*, *13*, 73.

Chen, Y., Xiao, W., Wang, Y., Liu, H., Li, X., & Yuan, Y. (2016). Lycopene overproduction in Saccharomyces cerevisiae through combining pathway engineering with host engineering. *Microbial cell factories*, *15*, 113.

Chow, J., Dionne, H. M., Prabhakar, A., Mehrotra, A., Somboonthum, J., Gonzalez, B., Edgerton, M., & Cullen, P. J. (2019). Aggregate filamentous growth responses in yeast. *mSphere*, *4*(2), e00702–18.

Crampin, H., Finley, K., Gerami-Nejad, M., Court, H., Gale, C., Berman, J., & Sudbery, P. (2005). *Candida albicans* hyphae have a Spitzenkörper that is distinct from the polarisome found in yeast and pseudohyphae. *Journal of Cell Science*, *118*, 2935–2947.

Cullen, P. J., & Sprague, G. F., Jr. (2000). Glucose depletion causes haploid invasive growth in yeast. *Proceedings of the National Academy of Sciences of the United States of America*, *97*, 13619–13624.

Czajka, J. J., Nathenson, J. A., Benites, V. T., Baidoo, E. E. K., Cheng, Q., Wang, Y., & Tang, Y. J. (2018). Engineering the oleaginous yeast *Yarrowia lipolytica* to produce the aroma compound β-ionone. *Microbial Cell Factories*, *17*, 136.

Doench, J. G., Hartenian, E., Graham, D. B., Tothova, Z., Hegde, M., Smith, I., Sullender, M., Ebert, B. L., Xavier, R. J., & Root, D. E. (2014). Rational design of highly active sgRNAs for CRISPR-Cas9-mediated gene inactivation. *Nature Biotechnology*, *32*, 1262–1267.

Fang, M., Ren, H., Liu, J., Cadigan, K. M., Patel, S. R., & Dressler, G. R. (2009). Drosophila ptip is essential for anterior/posterior patterning in development and interacts with the PcG and trxG pathways. *Development*, *136*, 1929–1938.

Fickers, P., Destain, J., & Thonart, P. (2009). Improvement of *Yarrowia lipolytica* lipase production by fed-batch fermentation. *Journal of Basic Microbiology*, *49*, 212–215.

Gajdoš, P., Ledesma-Amaro, R., Nicaud, J.-M., Čertík, M., & Rossignol, T. (2016). Overexpression of diacylglycerol acyltransferase in *Yarrowia lipolytica* affects lipid body size, number and distribution. *FEMS Yeast Research*, *16*(6). https://doi.org/10.1093/femsyr/fow062

Gancedo, J. M. (2001). Control of pseudohyphae formation in *Saccharomyces cerevisiae*. *FEMS Microbiology Reviews*, *25*, 107–123.

Gimeno, C. J., Ljungdahl, P. O., Styles, C. A., & Fink, G. R. (1992). Unipolar cell divisions in the yeast *S. cerevisiae* lead to filamentous growth: Regulation by starvation and RAS. *Cell*, *68*, 1077–1090.

Harvey, L. M., & McNeil, B. (1994). *Liquid fermentation systems and product recovery of* Aspergillus (pp. 141–176). Springer US.

Hirschhorn, J. N., Brown, S. A., Clark, C. D., & Winston, F. (1992). Evidence that SNF2/SWI2 and SNF5 activate transcription in yeast by altering chromatin structure. *Genes and Development*, *6*, 2288–2298.

Kawasse, F. M., Amaral, P. F., Rocha-Leão, M. H. M., Amaral, A. L., Ferreira, E. C., & Coelho, M. A. Z. (2003). Morphological analysis of *Yarrowia lipolytica* under stress conditions through image processing. *Bioprocess and Biosystems Engineering*, *25*, 371–375.

Kiss, E., Hegedüs, B., Virágh, M., Varga, T., Merényi, Z., Kószó, T., Bálint, B., Prasanna, A. N., Krizsán, K., Kocsubé, S., Riquelme, M., Takeshita, N., & Nagy, L. G. (2019). Comparative genomics reveals the origin of fungal hyphae and multicellularity. *Nature Communications*, *10*, 4080.

Konzock, O., & Norbeck, J. (2020). Deletion of MHY1 abolishes hyphae formation in *Yarrowia lipolytica* without negative effects on stress tolerance. *PLoS One*, *15*, e0231161.

Lee, B. N., & Elion, E. A. (1999). The MAPKKK Ste11 regulates vegetative growth through a kinase cascade of shared signaling components. *Proceedings of the National Academy of Sciences of the United States of America*, *96*, 12679–12684.

Li, M., Li, Y.-Q., Zhao, X.-F., & Gao, X.-D. (2014). Roles of the three Ras proteins in the regulation of dimorphic transition in the yeast *Yarrowia lipolytica*. *FEMS Yeast Research*, *14*, 451–463.

Li, Z. J., Shukla, V., Wenger, K., Fordyce, A., Pedersen, A. G., & Marten, M. (2002). Estimation of hyphal tensile strength in production-scale *Aspergillus* oryzae fungal fermentations. *Biotechnology and Bioengineering*, *77*, 601–613.

Löbs, A.-K., Schwartz, C., & Wheeldon, I. (2017). Genome and metabolic engineering in non-conventional yeasts: Current advances and applications. *Synthetic and Systems Biotechnology*, *2*, 198–207.

Magnan, C., Yu, J., Chang, I., Jahn, E., Kanomata, Y., Wu, J., Zeller, M., Oakes, M., Baldi, P., & Sandmeyer, S. (2016). Sequence assembly of *Yarrowia lipolytica* strain W29/CLIB89 shows transposable element diversity. *PLoS One*, *11*, e0162363.

Martin, S. M., & Bushell, M. E. (1996). Effect of hyphal micromorphology on bioreactor performance of antibiotic-producing *Saccharopolyspora erythraea* cultures. *Microbiology*, *142*, 1783–1788.

Morgunov, I. G., Kamzolova, S. V., Perevoznikova, O. A., Shishkanova, N. V., & Finogenova, T. V. (2004). Pyruvic acid production by a thiamine auxotroph of *Yarrowia lipolytica*. *Process Biochemistry*, *39*, 1469–1474.

Mösch, H. U., & Fink, G. R. (1997). Dissection of filamentous growth by transposon mutagenesis in *Saccharomyces cerevisiae*. *Genetics*, *145*, 671–684.

Mösch, H. U., Roberts, R. L., & Fink, G. R. (1996). Ras2 signals via the Cdc42/Ste20/mitogen-activated protein kinase module to induce filamentous growth in *Saccharomyces cerevisiae*. *Proceedings of the National Academy of Sciences of the United States of America*, *93*, 5352–5356.

Müller, C., Hansen, K., Szabo, P., & Nielsen, J. (2003). Effect of deletion of chitin synthase genes on mycelial morphology and culture viscosity in *Aspergillus* oryzae. *Biotechnology and Bioengineering*, *81*, 525–534.

Pan, X., & Heitman, J. (2002). Protein kinase A operates a molecular switch that governs yeast pseudohyphal differentiation. *Molecular and Cellular Biology*, *22*, 3981–3993.

Parveen, S., Singh, S., & Komath, S. S. (2019). *Saccharomyces cerevisiae* Ras2 restores filamentation but cannot activate the first step of GPI anchor biosynthesis in *Candida albicans*. *Biochemical and Biophysical Research Communications*, *517*, 755–761.

Patterson, K., Yu, J., Landberg, J., Chang, I., Shavarebi, F., Bilanchone, V., & Sandmeyer, S. (2018). Functional genomics for the oleaginous yeast *Yarrowia lipolytica*. *Metabolic Engineering*, *48*, 184–196.

Pomraning, K. R., Bredeweg, E. L., Kerkhoven, E. J., Barry, K., Haridas, S., Hundley, H., LaButti, K., Lipzen, A., Yan, M., Magnuson, J. K., Simmons, B. A., Grigoriev, I. V., Nielsen, J., & Baker, S. E. (2018). Regulation of yeast-to-hyphae transition in *Yarrowia lipolytica*. *mSphere*, *3*(6). https://doi.org/10.1128/mSphere.00541-18

Ramesh A, Ong T, Garcia JA, Adams J, Wheeldon I. 2020. Guide RNA engineering enables dual purpose CRISPR-Cpf1 for simultaneous gene editing and gene regulation in. *ACS Synthetic Biology*. *9*:967–971

Reis, V. R., Bassi, A. P. G., da Silva, J. C. G., & Ceccato-Antonini, S. R. (2013). Characteristics of *Saccharomyces cerevisiae* yeasts exhibiting rough colonies and pseudohyphal morphology with respect to alcoholic fermentation. *Brazilian Journal of Microbiology*, *44*, 1121–1131.

Ruiz-Herrera, J., & Sentandreu, R. (2002). Different effectors of dimorphism in *Yarrowia lipolytica*. *Archives of Microbiology*, *178*, 477–483.

Sabra, W., Bommareddy, R. R., Maheshwari, G., Papanikolaou, S., & Zeng, A.-P. (2017). Substrates and oxygen dependent citric acid production by *Yarrowia lipolytica*: Insights through transcriptome and fluxome analyses. *Microbial Cell Factories*, *16*, 78.

Schwartz, C., Cheng, J.-F., Evans, R., Schwartz, C. A., Wagner, J. M., Anglin, S., Beitz, A., Pan, W., Lonardi, S., Blenner, M., Alper, H. S., Yoshikuni, Y., & Wheeldon, I. (2019). Validating genome-wide CRISPR-Cas9 function improves screening in the oleaginous yeast *Yarrowia lipolytica*. *Metabolic Engineering*, *55*, 102–110.

Schwartz, C., Curtis, N., Löbs, A.-K., & Wheeldon, I. (2018). Multiplexed CRISPR activation of cryptic sugar metabolism enables *Yarrowia lipolytica* growth on cellobiose. *Biotechnology Journal*, *13*, e1700584.

Schwartz, C., Frogue, K., Misa, J., & Wheeldon, I. (2017). Host and pathway engineering for enhanced lycopene biosynthesis in *Yarrowia lipolytica*. *Frontiers in Microbiology*, *8*, 2233.

Schwartz, C., Frogue, K., Ramesh, A., Misa, J., & Wheeldon, I. (2017). CRISPRi repression of nonhomologous end-joining for enhanced genome engineering via homologous recombination in *Yarrowia lipolytica*. *Biotechnology and Bioengineering*, *114*, 2896–2906.

Schwartz, C., Shabbir-Hussain, M., Frogue, K., Blenner, M., & Wheeldon, I. (2017). Standardized markerless gene integration for pathway engineering in *Yarrowia lipolytica*. *ACS Synthetic Biology*, *6*(3). 402–409. https://doi.org/10.1021/acssynbio.6b00285

Schwartz, C. M., Hussain, M. S., Blenner, M., & Wheeldon, I. (2016). Synthetic RNA polymerase III promoters facilitate high-efficiency CRISPR-Cas9-mediated genome editing in *Yarrowia lipolytica*. *ACS Synthetic Biology*, *5*, 356–359.

Shama, S., Kirchman, P. A., Jiang, J. C., & Jazwinski, S. M. (1998). Role of RAS2 in recovery from chronic stress: Effect on yeast life span. *Experimental Cell Research*, *245*, 368–378.

Sudbery, P., Gow, N., & Berman, J. (2004). The distinct morphogenic states of *Candida albicans*. *Trends in Microbiology*, *12*, 317–324.

Szabo, R. (1999). Dimorphism in *Yarrowia lipolytica*: Filament formation is suppressed by nitrogen starvation and inhibition of respiration. *Folia Microbiologica*, *44*, 19–24.

Tisi, R., Belotti, F., & Martegani, E. (2014). Yeast as a model for Ras signalling. *Methods in Molecular Biology*, *1120*, 359–390.

Vallejo, J. A., Sánchez-Pérez, A., Martínez, J. P., & Villa, T. G. (2013). Cell aggregations in yeasts and their applications. *Applied Microbiology and Biotechnology*, *97*, 2305–2318.

Wang, K., Shi, T.-Q., Wang, J., Wei, P., Ledesma-Amaro, R., & Ji, X.-J. (2022). Engineering the lipid and fatty acid metabolism in for sustainable production of high oleic oils. *ACS Synthetic Biology*, *11*, 1542–1554.

Worland, A. M., Czajka, J. J., Li, Y., Wang, Y., Tang, Y. J., & Su, W. W. (2020). Biosynthesis of terpene compounds using the non-model yeast *Yarrowia lipolytica*: Grand challenges and a few perspectives. *Current Opinion in Biotechnology*, *64*, 134–140.

Xue, Z., Sharpe, P. L., Hong, S.-P., Yadav, N. S., Xie, D., Short, D. R., Damude, H. G., Rupert, R. A., Seip, J. E., Wang, J., Pollak, D. W., Bostick, M. W., Bosak, M. D., Macool, D. J., Hollerbach, D. H., Zhang, H., Arcilla, D. M., Bledsoe, S. A., Croker, K., McCord, E. F., Tyreus, B. D., Jackson, E. N., & Zhu, Q. (2013). Production of omega-3 eicosapentaenoic acid by metabolic engineering of *Yarrowia lipolytica*. *Nature Biotechnology*, *31*, 734–740.

Zacharioudakis, I., Papagiannidis, D., Gounalaki, N., Stratidaki, I., Kafetzopoulos, D., & Tzamarias, D. (2017). Ras mutants enhance the ability of cells to anticipate future lethal stressors. *Biochemical and Biophysical Research Communications*, *482*, 1278–1283.

Zhu, Q., & Jackson, E. N. (2015). Metabolic engineering of *Yarrowia lipolytica* for industrial applications. *Current Opinion in Biotechnology*, *36*. https://doi.org/10.1016/j.copbio.2015.08.010

SUPPORTING INFORMATION

Additional supporting information can be found online in the Supporting Information section at the end of this article.

How to cite this article: Lupish, B., Hall, J., Schwartz, C., Ramesh, A., Morrison, C., & Wheeldon, I. (2022). Genome-wide CRISPR-Cas9 screen reveals a persistent null-hyphal phenotype that maintains high carotenoid production in *Yarrowia lipolytica*. *Biotechnology and Bioengineering*, 119, 3623–3631. https://doi.org/10.1002/bit.28219